Journal of Environmental Management 383 (2025) 125189



Contents lists available at ScienceDirect

Journal of Environmental Management

journal homepage: www.elsevier.com/locate/jenvman



Research article

Resolving the climate-controlled hydrological regime in a model permafrost catchment for future management strategies

Łukasz Stachnik [a,b,*], Krzysztof Migała [a], Mirosław Wąsik [a], Henryk Marszałek [a], Aleksandra Wołoszyn [a], Marek Kasprzak [a], Elżbieta Łepkowska [c], Natalia Pilguj [d], Dariusz Ignatiuk [c,e], Anna Zielonka [f], Maciej Bartosiewicz [g]

[a] Faculty of Earth Sciences and Environmental Management, University of Wrocław, Wojciecha Cybulskiego 30, 50-205, Wrocław, Poland
[b] GFZ Helmholtz Centre, Potsdam, Telegrafenberg, 14473, Potsdam, Germany
[c] University of Silesia in Katowice, Institute of Earth Sciences, Będzińska Str. 60, 41-200, Sosnowiec, Poland
[d] Institute of Meteorology and Water Management, National Research Institute, Podleśna 61, 01-673, Warszawa, Poland
[e] Svalbard Integrated Arctic Earth Observing System (SIOS), SIOS Knowledge Centre, Svalbard Science Centre, P.O. Box 156, Longyearbyen, N-9171, Norway
[f] Institute of Nature Conservation, Polish Academy of Sciences, al. Adama Mickiewicza 33, 31-120, Kraków, Poland
[g] Department of Polar and Marine Research, Institute of Geophysics Polish Academy of Sciences, Księcia Janusza Str. 64, 01-452, Warszawa, Poland

A B S T R A C T

Climate change influences worldwide freshwaters with the most prominent effects in the Arctic and Alpine regions. Environmental management in proglacial zones underlain by permafrost requires understanding of hydrological regimes and water retention patterns. However, there is limited long-term data on the catchment-scale freshwater flow and retention for ecosystems within the continuous permafrost zones. Here, we characterized the hydrometeorological controls on the glacial-fluvio-lacustrine regime in a model Arctic catchment (SW Svalbard) to inform contingency plans for regions endangered by glacial-floods and permafrost landslides. We compiled a comprehensive hydro-meteorological dataset between 2005 and 2019 from a larger database (1972–2019) and applied bootstrapping, random forest, and multiple regressions, to elucidate the relationships between drivers (temperatures, sunshine duration, precipitation) and the intensity of freshwater flows. The hydrology exhibits strong seasonality with a pronounced peak between June and July controlled by precipitation ($R = 0.56$). From August to September, low-to-intermediate freshwater discharge is controlled by interactive effects of air temperatures and precipitation ($R = 0.71$). The interaction between hydrometeorology and catchment-scale discharge is stronger for August and September compared to June and July. The strongest warming trend between August and September (1979–2019) makes this period particularly relevant with regards to the long-term changes and environmental management in the permafrost-underlain catchments. Indeed, our northern hemisphere meta-analysis ($n = 1975$) revealed that majority of glacial floods (51 %) occurs at that time. We argue that permafrost management should include monitoring of surface temperature, precipitation and snow cover enabling establishment of stabilizing infrastructure in sensitive regions whenever threshold values are exceeded (i.e., Tmin >4 °C; P > 30 mm) and discharges increase.

1. Introduction

Climate change affects distribution and availability of global freshwaters with important consequences for populations and ecosystems (Qin et al., 2020; Sterling et al., 2013; Vörösmarty et al., 2010). These effects are particularly pronounced at high latitudes where warming is faster than the global average (i.e., "polar amplification"; (England et al., 2021). In the Arctic, rapid warming is coupled to shifts in precipitation leading to the intensification of the hydrological cycle (McCrystall et al., 2021; Rawlins and Karmalkar, 2024). Fast increase in the volume of free-flowing water through the permafrost-underlain catchments can stimulate cryosphere erosion leading to abrupt mass transport into the downstream ecosystems (Beel et al., 2018, 2020; Lehmann-Konera et al., 2017), increased emissions, landslides and glacial floods (Robison et al., 2023; Vonk et al., 2015). Intensification of the hydrological cycle also enables more efficient heating in the newly formed wetlands and expanding open water bodies (i.e., talik formation). The increase in the free-flowing water volume represents a positive feedback effect on the "polar amplification" enhancing glacier and permafrost thawing, as well as significantly increasing the risk

* Corresponding author. Faculty of Earth Sciences and Environmental Management, University of Wrocław, Wojciecha Cybulskiego 30, 50-205, Wrocław, Poland.
E-mail addresses: Lukasz.Stachnik@uwr.edu.pl (Ł. Stachnik), krzysztof.migala@uwr.edu.pl (K. Migała), miroslaw.wasik@uwr.edu.pl (M. Wąsik), henryk.marszalek@uwr.edu.pl (H. Marszałek), aleksandra.woloszyn@uwr.edu.pl (A. Wołoszyn), marek.kasprzak@uwr.edu.pl (M. Kasprzak), elzbieta.majchrowska@us.edu.pl (E. Łepkowska), natalia.pilguj@imgw.pl (N. Pilguj), dariusz.ignatiuk@us.edu.pl (D. Ignatiuk), zielonka@iop.krakow.pl (A. Zielonka), maciej.bartosiewicz@igf.edu.pl (M. Bartosiewicz).

https://doi.org/10.1016/j.jenvman.2025.125189
Received 16 September 2024; Received in revised form 5 March 2025; Accepted 29 March 2025
Available online 22 April 2025
0301-4797/© 2025 The Authors. Published by Elsevier Ltd. This is an open access article under the CC BY license (http://creativecommons.org/licenses/by/4.0/).

associated with glacial lake outburst floods (GLOFs (Harrison et al., 2018), and permafrost landslides (Huggel et al., 2012).

Changing climate influences the hydrological cycle in the Arctic and Alpine regions on the long and short timeframe (Beniston et al., 2018; Feng et al., 2021). Long-term effects include consequences of increasing temperatures on ice cover duration and rain-to-snow events (Graham et al., 2017; Wickström et al., 2020). Short-term effects include consequences of extreme weather events such as heavy springtime rainfalls and heat waves (Dobricic et al., 2020; Nakamura and Sato, 2022). However, in the context of the increasing frequency of extreme precipitation events and accelerating warming, there is limited information on the direct influence of seasonal temperature and precipitation variability on the hydrological cycle intensity in glacierized catchments underlain by permafrost. Existing analyses evidence a general trend towards increasing summertime runoff, related to frequent and heavy rainfalls (Lewis et al., 2012; Sund, 2008; Young et al., 2015). These trends correspond to the reported increase in autumnal air temperatures and rainfalls throughout the Arctic (Førland et al., 2011; Serreze et al., 2015; Wawrzyniak and Osuch, 2020). Seasonality of warming and precipitation patterns may influence soil water content and stability of glacial lakes. These effects can trigger more intense and frequent glacial floods and/or permafrost landslides, endangering millions of people (Taylor et al., 2023).

Despite the growing access to the continuous meteorological data from polar regions, interannual and multi-seasonal analyses that functionally link hydrological and meteorological effects in glacierized catchments are still scarce (Lafrenière and Lamoureux, 2019; Wang et al., 2022). Even fewer studies focus on High Arctic, where polar amplification is the strongest thus facilitating intense transitions in the hydrological cycle (Beel et al., 2021). Limited availability of long-term hydrological datasets and analyses (Lafrenière and Lamoureux, 2019; Nowak et al., 2021) constrains our ability to accurately forecast the future water regimes, where the rapid environmental change may lead to increased runoff (Lewis et al., 2012; Sund, 2008), peak greenhouse gases (GHG) emissions, floods, and landslides. These effects will potentially further stimulate ice and permafrost degradation, triggering an increase in the baseflow (Evans et al., 2015, 2020; Lamhonwah et al., 2017; Wang et al., 2023), water storage (Walvoord and Striegl, 2007; Walvoord and Kurylyk, 2016), and mass movements of both soil and ice (Owczarek et al., 2020; Zastruzny et al., 2023).

While accelerated thawing feeds streams and ponds resulting in surface water expansion, improved hydrological connectivity may enhance surface drainage, particularly in regions where riverine systems become better connected as the ice declines. This effect can influence the water content and flows throughout the active layer (Lamontagne-Hallé et al., 2018). Processes controlling the water content in the permafrost zone will reflect on the biogeochemical and geomorphological conditions. These changes can lead to higher productivity (Owczarek et al., 2021; Pedersen et al., 2022, Przytulska et al., 2017) and more reduced conditions during organic matter respiration (Robison et al., 2023) along with reduced permafrost stability enabling glacial floods and landslides (Westoby et al., 2014). Such water-driven relationships and potential feedbacks will be crucial to understand Arctic biomes under climatic transition and strategize for their future management. Considering knowledge gaps outlined above and the need to improve environmental models, we aimed to characterize the impact of hydrometeorological conditions on the freshwater regime in a model permafrost-underlain glacierized catchment, where ice decline leads to rapid freshwater expansion.

We hypothesize that water discharge is controlled by the ambient meteorological conditions during the rainfall-dominated part of the year rather than during the snow-dominated part. We determined the impact of hydrological connectivity, including change of lake volume, using interannual variability in matured High Arctic model systems during a period of 16 years of observations (1972–2019). This work provides characteristics of the water cycle in the rapidly changing high Arctic environment (Beel et al., 2021; Schmidt et al., 2023; van Pelt et al., 2019) thus provides process understanding urgently needed for improved glacial flood and mass movement forecasting (Emmer et al., 2022) and management strategies in remote polar and alpine regions (Vonk et al., 2023).

2. Study site

2.1. Local settings

The Brattegg River drains a small Arctic catchment (hereafter Bratteggdalen, 7.25 km^2) situated on Wedel Jarlsberg Land in SW Spitsbergen at an altitudinal difference of ~620 m (645–24 m above sea level, hereafter a.s.l.) (Fig. 1). This model catchment, typical for SW Spitsbergen, is constrained by mountain ridges and marine terraces (Migała et al., 2013). The bedrock consists of metamorphic rocks, including Precambrian and Lower Palaeozoic amphibolites, mica-schists, and quartzites (Czerny et al., 1992a, 1992b; Marszałek and Górniak, 2017). The catchment is well weathered while the talus slopes and moraines have been reworked by periglacial processes (Korabiewski, 2023; Owczarek et al., 2014; Senderak and Wąsowski, 2016). The upper terminus contains a relatively small (Wołoszyn and Kasprzak, 2023) cirque glacier Bratteggbreen (0.28km^2), that has lost about 47 % of its mass since 1936 (Owczarek et al., 2014), while declining by up to 68 % since Little Ice Age (Wołoszyn and Kasprzak, 2023). The decline of the Bratteggbreen, has been largely enhanced by an intense subaqueous melt events (Szponar, 1989). Rapid glacier decline, resulted in formation of three interconnected lakes with a total area of 0.24 km^2 in the lower part of the catchment (Marszałek and Wąsik, 2013). Importantly, the Bratteggbreen catchment is underlain by continuous permafrost (Kasprzak, 2015, 2020) that extends under the talus slopes near the largest Lake Myrktjørna (Senderak et al., 2017). The average thaw depth is estimated to reach 1.5 m at an altitude of 500 m (Brázdil et al., 1989; Kasprzak and Szymanowski, 2023) and has exceeded 3 m (max 20 m) on the elevated marine terraces forming the valley and the slope base affected by snowmelt and groundwater (Kasprzak and Szymanowski, 2023). The highest rates of thawing and subaqueous flows have been reported during the summer months (Kasprzak and Szymanowski, 2023).

2.2. Meteorology

The Bratteggdalen catchment is located in the vicinity of Stanisław Baranowski Polar Station (SBPS) (near the gauging station on Fig. 1); and less than 10 km from the Polish Polar Station Hornsund (PPS), where meteorological conditions are monitored continuously over the past 40 years (1979–2018) (Wawrzyniak and Osuch, 2019). For this period, mean annual air temperature at the PPS is −3.6 °C, with monthly means ranging from 4.6 °C in July to −10.2 °C in January. The mean daytime temperature is above 0 °C for an average of 124.5 days between June to September. For the same period, annual precipitation is 462.7 mm, where 27 % share (125 mm) is rainfall that occurs between June and August. In the period with above-zero air temperatures, the total precipitation is 199.9 mm (~43 % of annual mean). September and August are characterized by the highest precipitation values of 74.9 and 56.8 mm, respectively. Regarding snow cover, it typically occurs from the second half of September until early June (Górniak et al., 2016; Przybylak and Araźny, 2006). We assume here that despite certain local topo-climatic differences, the long-term meteorological data (1978–2019) recorded at PPS may be treated as representative for the weather conditions throughout the study area (Migała et al., 2013; Wawrzyniak et al., 2020; Wawrzyniak and Osuch, 2020). Meteorological measurements in the Bratteggdalen have been carried out intermittently since 1970, but often only in summer. Total precipitation is similar for PPS and SBPS (Migała et al., 2013). Year-round air temperature measurements show that the mean air temperature in summer

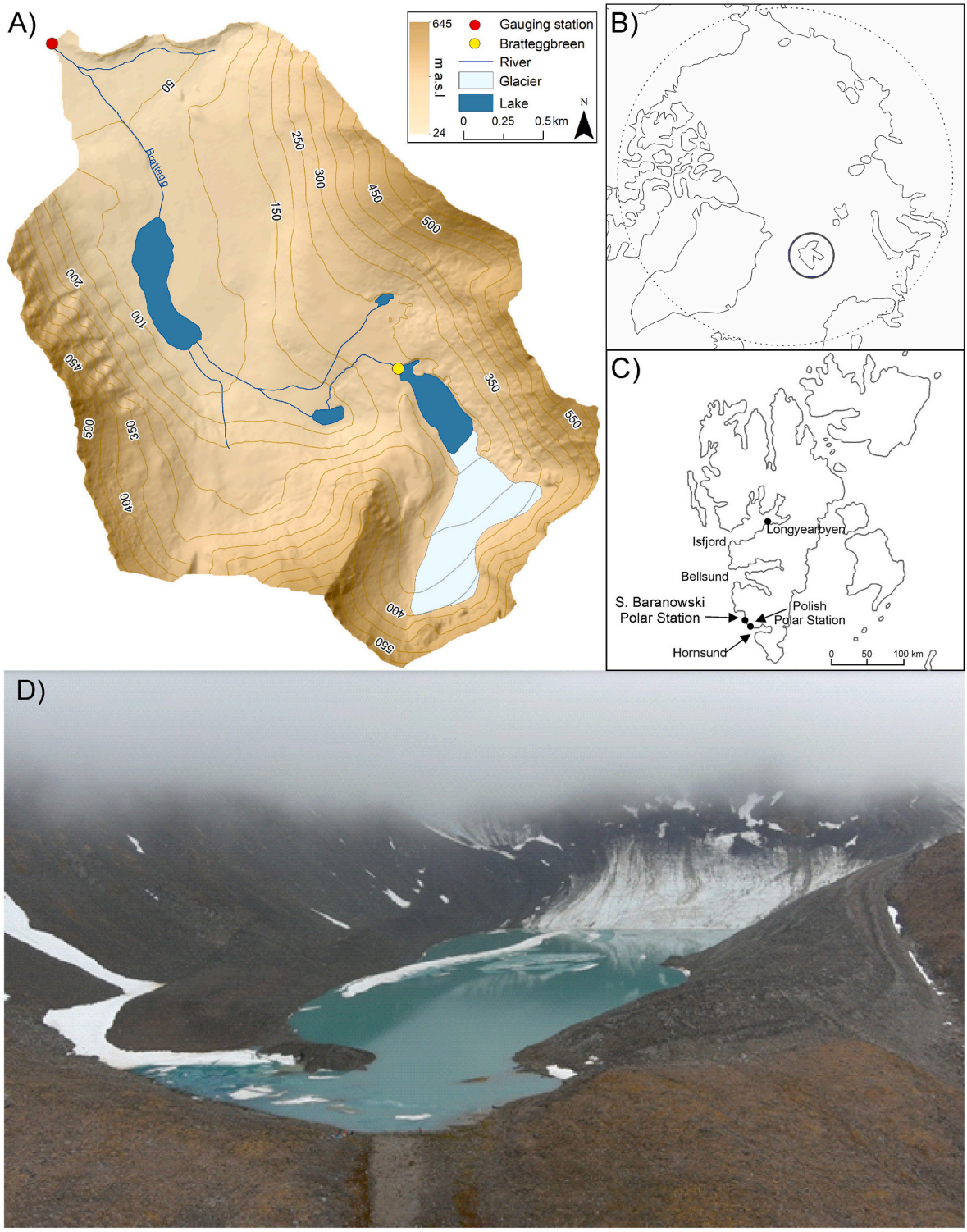


Fig. 1. (A) Study area of the Bratteggdalen catchment, (B) headwater part of catchment with glacial lake. Photo of the lake by Adam Nawrot (for Science Foundation).

(June–August) and winter (December–February) at SBPS is higher than at PPS by 0.9 and 0.4 °C, respectively (Migała et al., 2013, 2015).

3. Materials and methods

3.1. Hydrometeorological dataset

Hydrology of the Bratteggdalen catchment has been assessed at the gauging station located in its lower part (24 m a.s.l.) and complemented with a discrete sampling in the upper part (Fig. 1, Fig. A.1). Freshwater flow (also refered to as discharge) was calculated using the relationship between continous water level data and the discharge measured by the area-velocity method (Dobriyal et al., 2017). The water level was monitored with a set of atmosphere-calibrated pressure sensors located at the gauging station (Table A.1). For the analysis, data from the Bratteggdalen catchment were converted (Figs. A.2; A.3; A.4 and

supplemental Tables A2; A3) to weekly discharge rates. Weekly meteorological database (1979–2019) was prepared based on available daily PPS (WMO 01003) measurements, including 2-m air temperatures (minimum, maximum, average), precipitation measurments and sunshine duration data.

The hydrometeorological database, assembled to determine the relationship between the hydrological and meteorological conditions, includes the discharge and water temperatures, as well as the total precipitation data (corrected with elevation gradient) (Table 1). This database was completed with air temperature and sunshine duration obtained from the literature (Wawrzyniak and Osuch, 2019). Total precipitation rates were calculated as weekly sums (P_{week}) and averages (P_{av}); air temperatures were aggregated as the weekly means of the average, minimum, and maximum (T_{av}, T_{min}, T_{max}, respectively); water discharge and temperature were calculated as weekly means, i.e. Q_{av}, Q_{max}, Q_{min}, $WTMP_{av}$, $WTMP_{max}$, $WTMP_{min}$, respectively. The specific weekly runoffs (in mm) were calculated from the sum of daily runoff (in m^3), which was based on the average daily discharge (m^3/s) multiplied by day length (86400 secods), divided by catchment area in m^2 (R_{week}, hereafter "specific runoff").

Unique hydrological dataset for the Bratteggdalen catchment for 9 individual years (between 2005 and 2019) is explored in the analysis below. This dataset was complemented with historical hydrological data from the Bratteggdalen catchment for a total of 16 observation years (see Table A.1). The annual water budget was established using runoff and precipitation in warm (May–October, hereafter V-X) and cold periods (November–April, hereafter XI-IV), and the glacier ablation data. Direct runoff data (Table A.1) are complemented by modelled data from early summer and late autumn (Osuch et al., 2022). Precipitation data for winter (XI-IV) and summer (V-X), obtained from the Polish Polar Station (Migała et al. (2023), were corrected for elevation difference (19 %/100m, i.e., Nowak and Hodson (2013) and Majchrowska et al. (2015). Bratteggbreen ablation was estimated based on remote sensing data (see section 3.3 for details). We have also calculated runoff coefficients (C_{peak} and C_{event}), as the ratio of runoff to precipitation, for selected peak flow events during hydrologically active season betwee 2005 and 2019 (Eq. A.1, A.2, A.3).

3.2. Data analyses

In this study, we analyzed multi-annual hydrometeorological aspects of one of the longest data series for a High Arctic periglacial catchment (Nowak et al., 2021), using state-of-the-art statistical tools to establish the drivers of observed changes (Anghileri et al., 2014; Kundzewicz and Robson, 2004). All the data were grouped into representing either the snowmelt- (weeks of the year WOY, 23–29), and rainfall-dominated (WOY 30–37) periods. The multiannual changes of air temperature and precipitation for the investigated area, were presented using data from the PPS station, and the non-parametric Mann-Kendall two-tailed test, and Sen's slope estimator (*p-value* = 0.05) (Hipel and McLeod, 1994; Krogh and Pomeroy, 2018; Wawrzyniak and Osuch, 2020; Wilcox, 2001). The hydrometeorological relationships for non-normally distributed data were evaluated using non-parametric statistics (i.e., Spearman's rank correlation, hereafter *rho*).

Whenever the test assumptions (e.g., normality of residuals, lack of autocorrelation, constant variance) were met, we have determined the strenght of individual effects. For other variables, whenever the residuals of regression model were non-normally distributed, we log-transformed the data and used a non-linear regression analysis. Normality of residuals was tested using Kolomogorov-Smirnov with the Lilliefors modification (Eq. (A.4) and Shapiro-Wilk test (Eqs. A.5-A.7) (Kundzewicz and Robson, 2004). Autocorrelation of residuals was tested using the Durbin-Watson test (Savin and White, 1977). Whenever statistically sound, slopes of relationships and Pearson's correlation coefficients (hereafter *R*) were determined. Weekly means explained before, have been used to avoid serial autocorrelation throughout the dataset (Anghileri et al., 2014; Wawrzyniak et al., 2016). We also used random forest and bootstrapping methods (Adèr et al., 2008; Efron, 1979; Efron and Tibshirani, 1994) as well as a more robust linear regression approach to determine the functional relationships between hydrological (e.g., discharge, runoff) and meteorological conditions (e.g., air temperature, precipitation).

Random forest techniques adapted for non-normally distributed/colinear data (Breiman, 2001) were used to investigate interactions between Q_{avg} and environmental controls (see Table 2). We further quantified the contribution of individual predictors using the loss-decrease root mean square error (RMSE). All these analyses were performed using R packages (R Core Team, 2014) such as the 'boot' (Canty and Ripley, 2021; Davison and Hinkley, 1997), 'trend' (Pohlert, 2020), and 'caret' (Kuhn, 2008). In addition, the DALEX package was used for the visual explanation and exploration of the random forest models (Behrangi et al., 2015; Biecek, 2018; Dunn, 2001; Sharma and Tiwari, 2009).

3.3. Glacier ablation, proglacial lake volume and flood meta-analysis

The Bratteggbreen meltwater runoff was estimated following classical interpolation methods (Błaszczyk et al., 2019b; Ignatiuk et al., 2022). The calculation of the meltwater runoff in 2005–2010 and

Table 2
Performance of the random forest model for hydrological sub-periods during 2005–2019. RMSE, R, WOY denote root mean square error, coefficient of correlation, weeks of the year, respectively.

	RMSE	R
WOY 23–29	0.22	0.56
WOY 30–37	0.25	0.59
WOY 23–37	0.28	0.73

Table 1
Freshwater Discharges, total runoffs, glacier ablation rates in the Bratteggdalen during 2005–2019. Winter and summer precipitation totals corrected for altitude gradient (19 %/100 m) were used from meteorological station at the Polish Polar Station (following Migała et al., 2023). For the total runoff, discharge data were completed with model results (Osuch et al., 2022).

Year	Period of measurements (Date range & number of days)	Daily discharge [m^3/s] (mean, min-max)	Daily water temperature [°C] (mean, min-max)	Total runoff [10^6 m^3 (mm)]	Glacier ablation [10^6 m^3 (mm)]	Precipitation V-X [10^6 m^3 (mm)]	Precipitation XI-IV [10^6 m^3 (mm)]
2019	25.06 — 21.09 (89)	0.41 0.06–1.98	5.6 1.1–9.2	3.99 ± 0.24 (550)	0.32 ± 0.02 (44.3)	1.66 (229.3)	1.46 (283.1)
2018	18.06 — 08.09 (83)	0.77 0.2–1.77	5.1 1.8–8.6	7.25 ± 0.44 (1000.4)	0.5 ± 0.01 (69)	5.26 (726.1)	1.41 (273.4)
2017	22.06 — 23.08 (63)	0.57 0.09–1.98	4.0 0.4–8.1	8.07 ± 0.48 (1112.9)	0.54 ± 0.02 (74.9)	3.22 (443.7)	2.93 (566.9)
2010	13.06 — 25.08 (77)	0.71 0.14–2.46	3.9 0.3–7.5	6.87 ± 0.41 (947.3)	0.27 ± 0.01 (36.9)	2.69 (371.3)	2.1 (406.1)
2009	01.07 — 15.09 (77)	0.44 0.09–1.35	4.9 0.6–8.1	4.61 ± 0.28 (635.6)	0.39 ± 0.01 (54.4)	2.32 (319.9)	1.21 (233.9)
2008	25.06 — 26.09 (94)	0.84 0.03–3.66	3.3 0.1–5.7	7.02 ± 0.42 (968.5)	0.3 ± 0.01 (41.6)	2.92 (402.9)	1.2 (232.8)
2007	01.07 — 27.09 (89)	0.6 0.14–1.63	3.1 -0.2-6.8	5.55 ± 0.33 (765.7)	0.27 ± 0.01 (36.8)	2.65 (366.2)	1.45 (280.8)
2006	04.06 — 22.09 (111)	0.61 0.12–3.26	4.0 -0.2-7.5	5.96 ± 0.36 (822.2)	0.32 ± 0.01 (43.7)	2.68 (369.4)	1.73 (334.2)
2005	23.07 — 13.09 (53)	0.51 0.1–1.96	4.6 -0.2-5.8	4.08 ± 0.24 (563.1)	0.33 ± 0.01 (45.5)	2.59 (357.5)	1.39 (269.5)

2017–2019 was based on mass balance data from the Hansbreen and Werenskioldbreen glaciers, respectively (WGMS, 2020). Both glaciers are positioned within 10 km of the Bratteggbreen. The relationship between surface summer ablation and elevation for each ablation season was extrapolated to the Bratteggbreen using Digital Elevation Models (DEM, 50 m × 50 m resolution) with geoidal height (EGM2008) from the Pleiades high-resolution images taken on 20.08.2017 (Błaszczyk et al., 2019a). A DEM mosaic image from the Norwegian Polar Institute and filtered ASTER GDEM were used for the period between 2005 and 2010 (Moholdt et al., 2019), whereas the data from the ArcticDEM 7 were used for the period between 2017 and 2019 (Porter et al., 2018). The proglacial lake volume in the Brateggdalen was estimated using aerial photos of the lake surface between 1936 and 2020 as well as local topography data with 'lakemorpho' modelling package (Hollister and Stachelek, 2017). For the glacial flood seasonal frequency analysis, we have used monthly data from the Lützow et al. (2023) for floods reported throughout the north hemisphere.

4. Results

4.1. Long-term meteorological changes

Between 1979 and 2019, significant positive trends of air temperatures were observed (Fig. 2A). The observed changes in average and maximum air temperature for WOY 30–37 (0.38 °C and 0.42 °C per decade, respectively) were higher when compared to WOY 23–29 (i.e. 0.37 °C). The trend of minimum air temperature is the greatest, with a value of 0.45 °C per decade for both periods (WOY 23–29 and WOY 30–37). The sum of precipitation, increased significantly only for WOY 30–37, at an average rate of16.8 mm per decade (Fig. 2B).

4.2. Freshwater flows

Seasonal patterns of freshwater discharge, runoff and temperature showed a clear change during the summer. For WOY 23–27 (late June to mid-July), the mean daily discharge rates exceeded 0.4–0.6 m^3/s and snowmelt peak flows (>0.8 m^3/s) were stimulated by precipitation and warming (Fig. 3). For example, peak flow events in 2006 (two events: 18–19.06, 1–3.07) and 2019 (two events: 1–2.07 and 5–6.07) were usually related with extreme precipitation rates exceeding 15 mm (prior or during peak flow) and warming(e.g., heatwaves between 1–3.07.2006 and between 5–6.07.2019). During WOY 24–33 (late July to August), the discharge decreased markedly to low flow conditions (<0.4 m^3/s). During the summer-autumn transition (WOY 35–38; August to early September), the average discharge increased rapidly following intense rainfall (1–2 m^3/s, Fig. 3). Discharge in snowmelt-dominated part of the season was lower as compared to the rain-dominated periods (see Fig. 3B). A similar seasonal pattern with high weekly specific runoff (R_{week}) occured during snowmelt in spring/summer transition. Comparably elevated discharge during rain events during summer/autumn transition was observed for weekly data between 2005 and 2019 (Fig. 4A). R_{week} exceeded total precipitation during the snowmelt-dominated part of season as compared to the rain-dominated part when this difference was much less pronounced (Fig. 4B). Extreme events were observed in the later part of the season (after 29 WOY) when precipitation reached 80 mm and runoffs 176 mm as compared to averages of 8 and 30 mm, respectively.

4.3. Hydrometeorology

The analysis of freshwater discharge rates revealed differences between the snowmelt-dominated and rain-dominated datasets. Indeed, discharge rates were more closely correlated with air temperatures (T_{min} and T_{av}, respectively) (*rho* > 0.5) for the rainfall-dominated part of the season (WOY 30–37) compared to the snow-dominated part (WOY 23–29; (Table A.4). Early in the season (WOY 23–29), the maximum freshwater discharge (Q_{max}) correlated to the total and average precipitation rates (P_{week} and P_{av}, *p-value* < 0.05, *rho* > 0.35; Fig. A.5). Random forest and bootstrapping analyses revealed general and seasonal hydrometeorological effects. Indeed, models explaining Q_{av} demonstrated the strongest relationship for the entire period (WOY 23–37) ($R = 0.73$; root mean square error, RMSE = 0.28), indicating the crucial importance of the precipitation and water temperatures in controlling hydrology of the glacierized catchment (Fig. 5). When separated into two periods of the year (i.e. WOY 23–29 and WOY 30–37), models yield similar R and RMSE (Table 2), whereas predictors of changes for each of these periods are different. The most important drivers of hydrology in WOY 23–29 was precipitation (P_{week}). The analysis with the bootstrapping method revealed that P_{week} was more strongly correlated with Q_{max} (and to lesser extent with Q_{min}) reaching $R \sim 0.5$ (Fig. A.6). In contrast for WOY 30–37 it was the interactive effect of temperature and precipitation that (T_{min}, P_{week}, T_{av}) predicted Q_{av} (Fig. 5, Fig. A.6). This

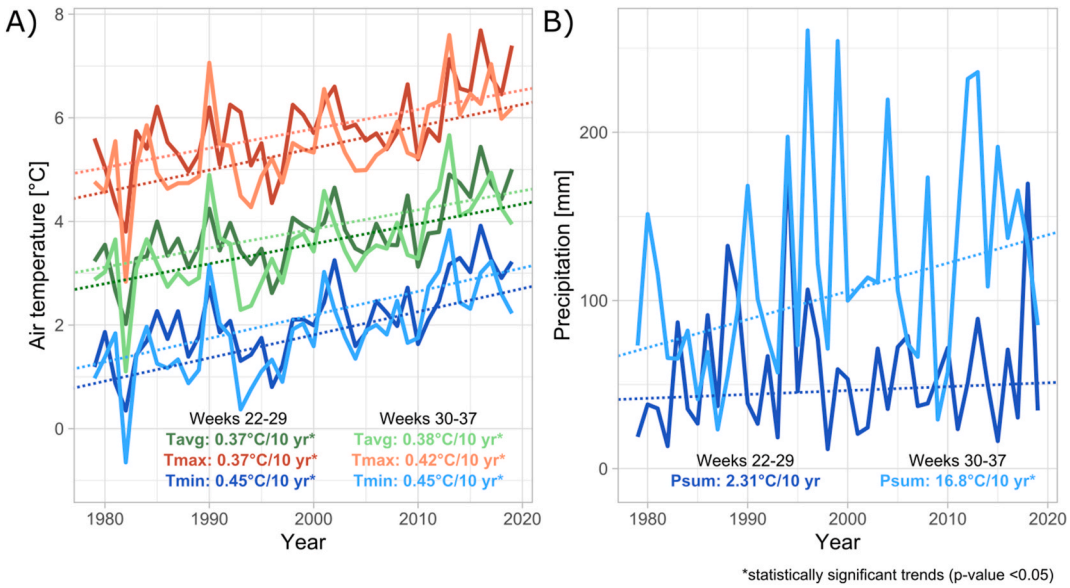


Fig. 2. Multiannual changes in meteorological parameters in 1979–2019: (A) 2-m air temperature at the Polish Polar Station, (B) total precipitation at the Polish Polar Station.

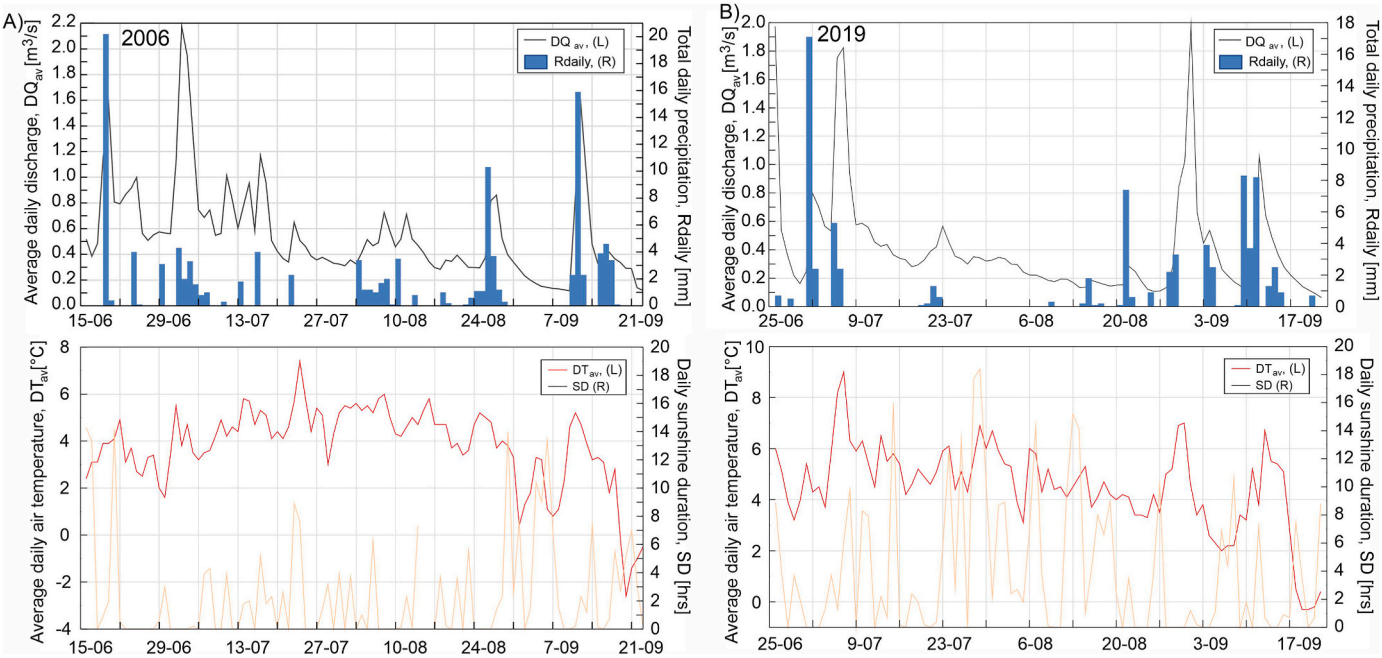


Fig. 3. Evolution of hydrological and meteorological conditions during the two exemplary ablation seasons: (A) 2006 snow-melt dominated with high discharge in the spring, (B) 2019 rain-dominated with high discharge in late summer/autumn transition.

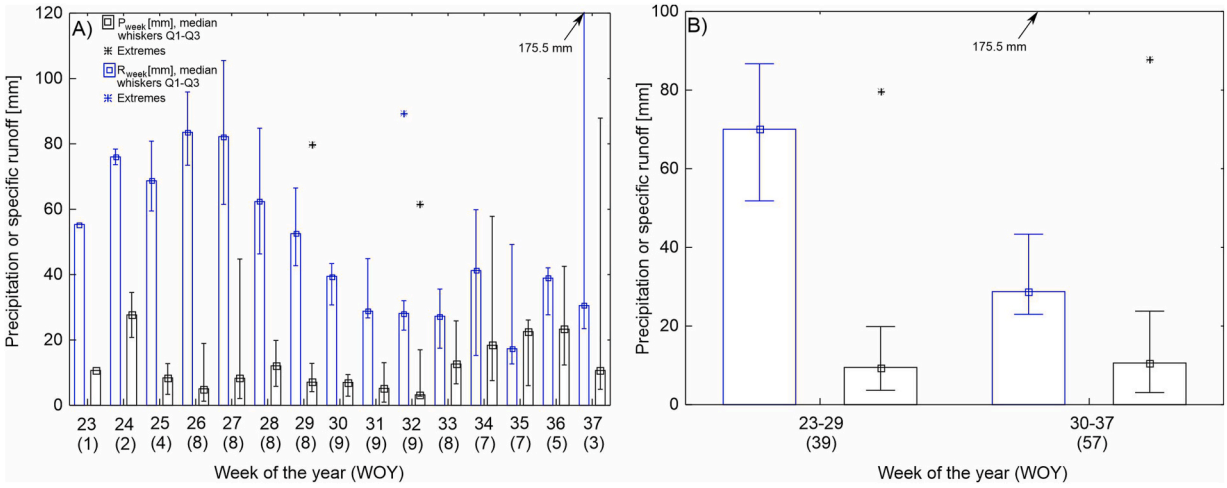


Fig. 4. Weekly aggregated specific runoffs and precipitation rates in Bratteggdalen catchment from 2005–2019: (A) each week from week 23 to week 37, two groups for weeks 23 –29, and (B) weeks 30 –37. Total numbers of weekly measurements are provided in parentheses.

is also in line with results from bootstrapping analysis, where both T_{min} and T_{av} show high correlation with Q_{min} (R~0.5) for WOY 30–37 (Fig. A.6 C).

For the non-linear regression analyses hydrological data were corrected with the logarithmic transformation to normalize distributions and remove any potential autocorrelations (Kundzewicz and Robson, 2004). Subsequently, the aggregated data for two periods (WOY 23–29 and WOY 30–37) correlated for $logQ_{max}$ vs. P_{week} and $logQ_{min}$ (and $logQ_{av}$) vs. T_{min}, respectively. For WOY 30–37, precipitation rates (P_{week} or P_{av}) were also marked as significant predictors (Table A.5). For WOY 23–29, non-linear regression showed a positive slope and correlation ($R > 0.5$) between $logQ_{max}$ and P_{week} (Fig. 6A). Conversely, there was no significant relationship (*rho* < 0.3) with air temperature (Table A.4). Specific freshwater discharge rates (Q_{min} and Q_{av}), correlated to T_{min} for the rain-dominated part of the season (WOY 30–37; *rho* >0.5) (Table A.4). In further support, this correlation was comparable to the Pearson's coefficients ($R \sim 0.5$) calculated using the bootstrap method (Fig. A.6). By including P_{week}, the Pearson's correlation coefficient increased to $R = 0.71$ (Fig. 6B). The bootstrap method for WOY 30–37 showed a stronger correlation with lower confidence intervals than WOY 23–29 weeks (Fig. A.6).

Similarly to weekly results, the correlation between monthly runoffs and total precipitation was stronger in the rain-dominated, than in the snowmelt-dominated part of the season ($R > 0.9$), particularly for the aggregated August–September data (similar period as for WOY 30–37, Fig. 7A). Parallel analysis for the months of June and July (WOY 23–29) revealed that this relationship is not significant.

4.4. Precipitation, glacier ablation and lake volume

Observational freshwater discharge data revealed that precipitation (summer and winter) was not significantly different from the specific

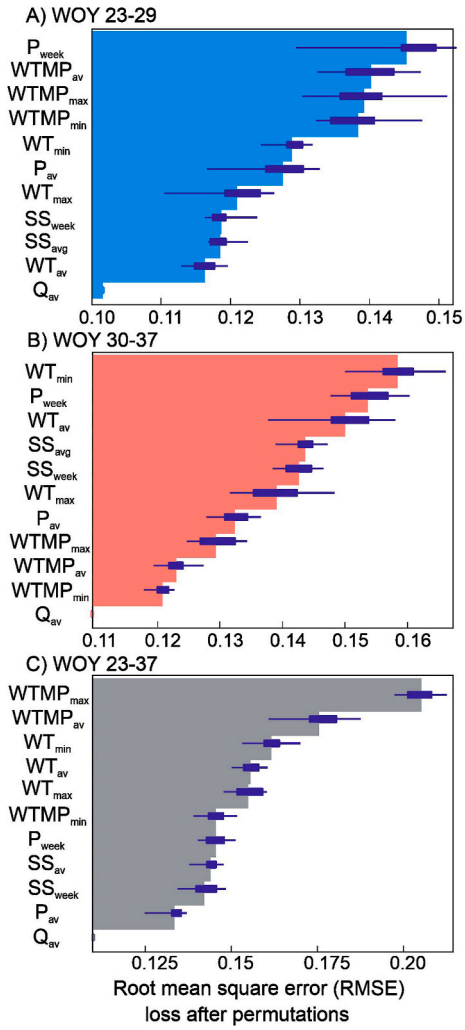


Fig. 5. Relationship between mean weekly discharge and other hydrometeorological parameters (e.g. water temperature, air temperature, total precipitation, sunshine duration) using the random forest: (A) from week 23 to week 37, (B) from week 30 to week 37, (C) from week 23 to week 37.

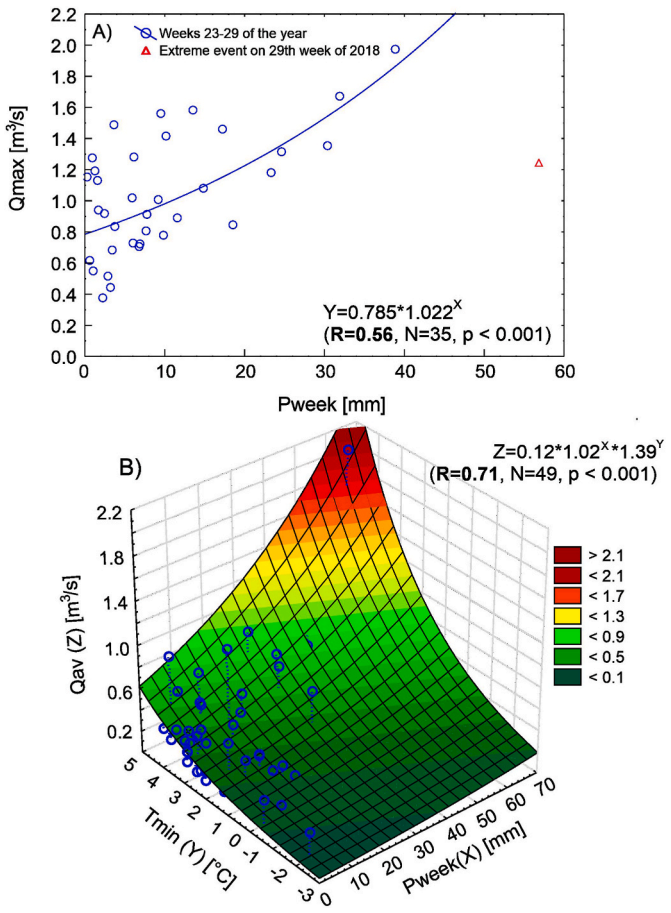


Fig. 6. Hydrometeorological relationship in the Bratteggdalen catchment for 2005–2019: (A) total precipitation and mean maximum discharge for weeks 23–29 of the year, and (B) mean minimum air temperature and total precipitation vs discharge for weeks 30 –37 of year. For details of the range of data available, see Tables 1 and A1.

runoff in the Bratteggdalen catchment (Table 1, Fig. 7B). Total runoff ranged from 3.99 to 8.07 $\times$ 10^6 m^3, corresponding to specific runoffs of 550.0 and 1112.9 mm, respectively. The total precipitation in summer and winter was lower compared to runoffs and ranged from 229.3 to 726.1 and from 165.8 to 403.7 mm, respectively. In most years, except for 2005, the sum of total summer and winter precipitation was lower than the annual runoff (Fig. 7B;Table 1). During ablation season, the average runoff was higher by 0.36 $\times$ 10^6 m^3 (range from −0.79 $\times$ 10^6 m^3 to 2.11 $\times$ 10^6 m^3) compared to the total precipitation (sum of snow and rain). Therefore, we estimate that glacier ablation contributed on the order of 10 % to the total catchment-wide freshwater discharge (see section 3.3). Glacier decline resulted in a rapid increase of the proglacial lake volume within Bratteggdalen from 0.3 $\times$ 10^4 m^3 in 1990 to 1.5 $\times$ 10^4 m^3 in 2020 (see aerial photo of the lake in 2023, Fig. 1). The probability of glacial lake flood increased significantly as the lake water level is now only <2m below the maximum ice dam height (personal observation).

5. Discussion

Our analyses show that the warming is more intense during the rainfall-as compared to the snowfall-dominated season (Fig. 2A). This seasonality was associated with increased precipitation during the warmer period (i.e., 17 mm per decade, see Wawrzyniak and Osuch, 2020). We also evidence that incresing temperature and precipitation enhance the freshwater drainage (Figs. 5, 6B and 7B). Whereas precipitation trends are rising strongly in the rainfall-dominated period during the last few decades, the overall runoff is consistently higher for the snowmelt-dominated period (see Fig. 4), which is similar with other permafrost underlain catchments in High Arctic (Killingtveit et al., 2003; Osuch et al., 2019; Wawrzyniak et al., 2020). Thus while our model catchement is experiencing a climate change-triggered transition, it still retains its orginal nival character. Overall, our study, by providing a comprehensive insights into multiannual hydrometeorology, contributes to understading of the ecosystem connectivity effects on the hydrology within a glaciarized permafrost catchments under rapid climate change in Svalbard and beyond (see Fig. 8 and Nowak et al., 2021).

5.1. Seasonally diverse hydrometeorological effects

We reveal a difference in the hydrometeorological relationships for the snowmelt- and rainfall-dominated parts of the season (Fig. 5). During the snowmelt-dominated period (weeks 23–29), rainfall events strongly enhanced discharge (Q_{max}; Figs. 5 and 6A). By contrast rising temperatures did not result in an immediate discharge increase early in the season (Fig. 5), but stimulated the snowmelt contribution to subsequent peak runoff. The effect of warming on the catchment-wide discharge is potentially delayed until snow-derived water reaches the river. Indeed, with the steady warming during that period, the runoff reaches its maximum only after the complete snowmelt. The water

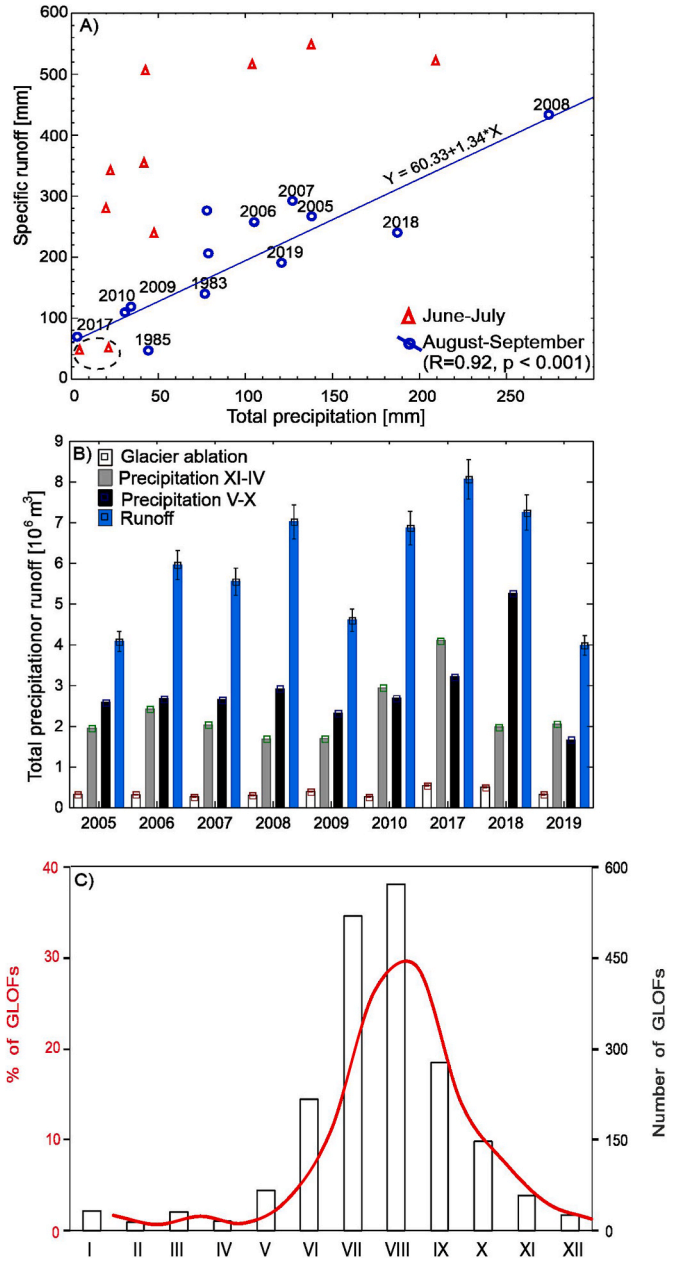


Fig. 7. (A) Relationship between precipitation corrected for elevation gradient at the Polish Polar Station and specific runoff in the Bratteggdalen during the ablation seasons in 1985–2019; note that the black dashed circle marks the years (1985, 2005) with datasets shorter than 10 days (metadata available in Table 1). (B) components of specific runoff in the Bratteggdalen between 2005 and 2019, and (C) seasonal frequency distribution (in % and as number of events) of glacial lake floods over the north hemisphere since 1638 (n = 1973; data available from https://zenodo.org/records/7330345).

retention within the snow cover and slow release of the snowmelt waters into streams and/or lakes (e.g., increase in the snow line altitude, thickening of the active layer) further delays the system's response to warming. These effects are contrasted by a strong response of the discharge rates to air temperature and precipitation later in the season (WOY 30–37; Figs. 5 and 6B). Such connectivity difference between the snow-vs rainfall-dominated periods control the influence of hydro-meteorological conditions on the freshwater budget.

Rainfall events lead to high discharges during the snowmelt-dominated part of the season, with runoffs exceeding precipitation. Interestingly, Q_{max} correlates to P_{week} and P_{av} (Figs. 5 and 6A),

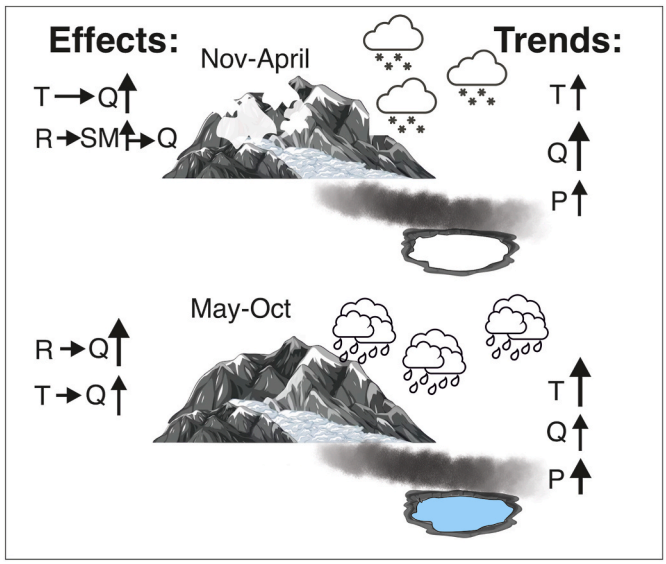


Fig. 8. Schematic illustration of the observed hydrological and meteorological effects for the model Brateggdalen catchment including patterns in temperature (T) discharge (Q), precipitation (P) as well as effects between warming, rainfall (R), snowmelt (SM) and discharge (Q) for the winter and summer observation periods. Size and direction of arrows is representative for the direction and magnitude of seasonal changes and interactions.

indicating that high discharge events are triggered by the rapid snowmelt that is accelerated by rainfall. The total runoffs during peak flows in July were several times higher than the total precipitation based on runoff coefficients, C_{peak} and C_{event} (Fig. A.7, Table A.6). Decline of the lake ice and breaking of snow dams in river channels further enhances water flows. During the year, when air temperatures consistently exceeded 0 °C, warming appears to have a relatively minor influence on the discharge events. The formation of a layer of ice within and beneath the snowpack, as a consequence of frequent rain-on-snow and snowmelt during winter-autumn (Łupikasza et al., 2019, 2021), is likely to have delayed water flows through and underneath the snowpack, leading to such a lagged response. Clearly, accelerated warming during the snowmelt period triggers peak discharge events (Young et al., 2015) as indicated by the relationship between T_{min} and discharge (Fig. 5A). However, such effects have not been observed in the longer-term dataset when the influence of snow accumulation and extreme precipitation events prevails in controlling discharge rates (Park et al., 2024; Wawrzyniak et al., 2020).

The decrease in the snow water equivalent and the snow cover duration results in shorter periods of peak discharge by mid–season (Hanssen-Bauer et al., 2019; Pelt and Kohler, 2015). This observation agrees well with results from other catchments in Arctic lowlands (Beel et al., 2018, 2021). Overall, the hydrological regime of our model High Arctic catchment over the past 25 years was strongly affected by the precipitation-induced peak discharge events during the snowmelt-dominated part of the season. These effects resulted in torrential discharges when a rapid precipitation increase was no longer buffered by the retention within the snow cover and/or in proglacial lakes (Serreze et al., 2021; Sobota et al., 2020).

Warming controls freshwater flows during the rainfall-dominated part of the summer. The correlative effect between T_{min} and discharge (Q_{av}, Q_{min}) was stronger as compared to direct precipitation effects (Fig. 5, Table A.4). The inclusion of P_{week} strengthened this relationship even further (R~0.7, Fig. 6B) as compared to that between T_{min} and Q_{min} (R~0.6, Table A.5). Pronounced effect of air temperature on hydro-meteorological conditions in the rainfall-dominated part of the season, is most likely related to the deepening of the active layer and/or permafrost (see (Wawrzyniak et al., 2016) and changes in the

catchment-wide water retention capacity after the snowmelt (e.g., quick response to rain events, see Fig. 7A). In consequence, discharge rates, reflecting baseflow conditions and water residence times, are strongly controlled by the (minimal) air temperatures (see review of recent studies in Table A.7). Strong correlation between air temperature and baseflow, as a consequence of deepening active layer, has been observed in catchment underlain by permafrost in Arctic Eurasia, Qinghai-Tibetan Plateau, Himalayas, Alaska (Singh et al., 2000; Sjöberg et al., 2021; Song et al., 2021; Wang et al., 2012; Zastruzny et al., 2024). Recent warming further increase groundwater flow, its contribution to total runoff, and water storage in active layer (Ge et al., 2011; Lin et al., 2020) as well as redistribution of soil moisture (Debolskiy et al., 2021). Impact of precipitation increase on discharge in the permafrost underlain catchment is less pronounced (Cooper et al., 2023; Singh et al., 2000) and is usually linked with high river flow events (Song et al., 2021).

The relatively weak direct relationship between rainfall and discharge stands in contrast to observations from other Arctic catchments where the increase in discharge was driven mostly by more frequent rainfalls and precipitation increase (Lewis and Lamoureux, 2010; Makarieva et al., 2019; Osuch et al., 2022; Stuefer et al., 2017; Young et al., 2015). However, this previous work also argues that rainfall-triggered thawing may elevate discharge later in the season (Caine, 2010). Our study expands this argument by showing that a rise in minimum air temperature facilitates such a process. Indeed, warming-enhanced hydrological connectivity throughout the active layer over the summer-to-autumn transitions likely enables a more efficient transfer of rainfall via the supra-permafrost flows within the active layer to river channels (Stachniak et al., 2022; Wąsik et al., 2023). To sum up, air temperature and more intense rainfalls accelerate active layer and/or permafrost deepening, leading to a long-term increase in the baseflow freshwater flow within a model catchment underlain by continuous permafrost (Fig. 6B). This may result in lower soil/rock stability and more frequent mass movements.

On a finer temporal scale, we have observed a strong relationship between precipitation and runoff in late summer (August and September, Fig. 7A). This corresponds with the reported summertime deepening of the active layer (Kasprzak, 2020; Kasprzak and Szymanowski, 2023) that is also apparent from other comparative studies in this region (Brázdil et al., 1988, 1989; Piasecki and Pulina, 1975). The strong link between surface air temperature and ground temperatures (down to 0.5 m, Kasprzak and Szymanowski (2023) supports the thermo-hydrological mechanism behind the discharge and raising T_{min} (Figs. 5 and 6B) and agrees with evidence that the mean annual air temperature stimulates baseflow (Evans et al., 2015; Wang et al., 2019, 2021). Our results provide evidence for a synergy between hydrometeorological processes and active layer thickness towards enhanced freshwater circulation in permafrost catchments.

5.2. Runoff components and perspective for ecosystem management

Overall glacial flow contributes about 10 % to catchment-wide freshwater runoff. This fraction reflects the glacier percentage area in the catchment and potential shading effects (see aerial photo on Fig. 1). The increase in runoff from the declining ice is buffered through the expanding proglacial lakes thus have limited immediate influence on the hydrology and permafrost stability. Currently, the ecosystem-scale water budget and soil water content are controlled rather by the supra-permafrost flows and water release from the annual snow cover. This conclusion is supported by the data showing that runoff frequently exceeds the total precipitation volume (on average by ~ 100 mm). Even when accounting for the evapotranspiration (~70 mm; Killingtveit et al., 2003), our data points to a relatively high freshwater discharge, most likely via enhanced supra-permafrost thawing and inflows.

Indeed, the catchment-specific runoffs are between 50 and 200 % higher compared to other Arctic regions with similar glacier cover (<15 % of total area) or similarly sized glacier-free basins (Jania and Pulina, 1994; Killingtveit et al., 2003). Runoff increases due to the unique climatic and hydrological conditions in the southern location of the study area, which is influenced by warm, humid maritime air masses. The West Spitsbergen Current brings about warming that accelerates release of water stored in glaciers and permafrost, leading to high surface water runoffs (Hanssen-Bauer et al., 2019). This evidences a considerable water sourcing from the underlaying permafrost. On the other hand, runoffs in Bratteggdalen are up to three times lower than these reported from the more strongly glacierized basins (Killingtveit et al., 2003; Majchrowska et al., 2015; Stachnik et al., 2016). Following these observations, we argue that the extent of water-driven ice decline shall have a major impact on the future of permafrost catchments. Data analyzed using the random forest method explained observed variability of the runoff relatively well (Sihag et al., 2021; Zounemat-Kermani et al., 2021), while alternative parametric linear regressions and, bootstrapping) can be considered as complementary tools to better understand the hydrometeorological changes (Alobaidi et al., 2021; Ghorbani et al., 2018; Zhou et al., 2018). Along these lines, future exploitation of artificial networks (Alobaidi et al., 2021; Ghorbani et al., 2018; Zhou et al., 2018) will enhance predictive models.

Our metanalysis of glacial lake floods over the north hemisphere revealed that most of these extreme events occurred in the rainfall rather than snowfall dominated part of the season (Fig. 7C). This agrees well with results showing higher freshwater flows in the latter part of the season, particularly when rainfall enhanced snowmelt. These observations provide a perspective for future plans to monitor, model and manage regions endangered by glacial floods. The global decline of snowfall (Bintanja and Andry, 2017; Li et al., 2020) as well as shift towards higher rainfall events (Bintanja and Andry, 2017) may play an important role in the timing and frequency of glacial floods. Monitoring and management programs should, therefore, focus on the transition periods when lakes are losing their ice while simultaneously receiving large volumes of water from their permafrost catchments. Along these lines, design of GLOF Early Warning Systems (An et al., 2022; Kumar et al., 2022) should focus not only on lake water level and glacial dam stability observations but include recording of discharge rates through the permafrost that contribute to major destabilizing effects (Kurylyk et al., 2016).

In this vein, the increase in supra-permafrost water content and flow can stimulate mass movement and landslides. Our data implies that multiannual hydrological observations can be used to established threshold values of temperature and precipitation (rainfall) when the buffering capacity of the permafrost is exceeded and when mass movements will become more probable. Indeed, hand-in-hand with climate change, these extreme events are becoming increasingly frequent throughout the permafrost regions and put infrastructure and developments at risk (Jakob, 2022). Previous work evidenced that water infiltrating downwards, can trigger slides when its transport is limited within the underlying ice/frozen soil (Shan et al., 2015). Our study broadens this perspective by showing that changes in the minimal temperature can have a decisive effect on permafrost stability. Increase in the baseflow and soil water content following higher T/T_{min} should be recognized as a proxy for the possible extreme mass movement. Considering that minimal temperatures are routinely monitored, modelling/forecasting of floods and mass movements using T_{min} as a readily available indicator of the permafrost stability that can be used to increase the accuracy of future predictions as well as to design and manage worldwide permafrost stabilization infrastructures.

6. Conclusions

Using our long-term dataset from a model arctic catchment we show a hydrological and meteorological influences on the water balance during rainfall- and snowmelt-dominated part of the year. Snowmelt gives rise to high freshwater discharges, and peak runoffs largely exceeding total precipitation. In contrast, minimum air temperatures

and to some extent, precipitation volume control the discharge events in the rainfall-dominated part of the season. Any increase in the active layer's thickness, by enhancing its hydrological connectivity and water retention potential, leads to accelerated water transfer downstream to rivers and lakes. Warming and intensified precipitation events in the rainfall-dominated part of the season can result in an overall increase of the freshwater flow through the permafrost catchments in the future. Indeed, our rich observational dataset provides basis for a more advanced hydrological modelling supported by the robust climate projections and functional relationships (e.g., CMIP6, Emergent Constraint approach). Such efforts will enable us to create a set of plausible scenarios for the high Arctic under different climate forcing (e.g., Chai et al., 2022; Hu et al., 2021; Zhu et al., 2023).

Understanding and predicting changes in the hydrology of permafrost catchments require an interdisciplinary approach, including a range of observational data and robust statistical analyses ideally supported by artificial networks. The combination of classical and novel techniques will enable more robust forecasting. Integration of the seasonal and interannual effects in permafrost hydrology, as well as accounting for processes triggering pulse discharges (i.e., high rainfalls to rapid snowmelts) will catalyze the design of more efficient systems for glacial flood risk monitoring. In populated or industrialized regions endangered by glacial floods and permafrost landslides early warning and management can save lives and infrastructure. In the future, when appropriate technology and data is available, energy from the glacial freshwater streams/mass movements during GLOFs can be re-directed to fuel electricity production or form potable water supplies.

CRediT authorship contribution statement

Łukasz Stachnik: Writing – original draft, Validation, Investigation, Data curation, Conceptualization. **Krzysztof Migała:** Methodology, Funding acquisition, Data curation, Conceptualization. **Mirosław Wąsik:** Investigation, Data curation. **Henryk Marszałek:** Supervision, Investigation, Funding acquisition. **Aleksandra Wołoszyn:** Writing – original draft, Visualization, Data curation. **Marek Kasprzak:** Writing – original draft, Funding acquisition, Data curation. **Elżbieta Łepkowska:** Methodology, Data curation. **Natalia Pilguj:** Visualization, Software, Methodology. **Dariusz Ignatiuk:** Investigation, Funding acquisition, Data curation. **Anna Zielonka:** Writing – original draft, Visualization, Methodology, Data curation. **Maciej Bartosiewicz:** Writing – original draft, Conceptualization.

Declaration of competing interest

The authors declare that they have no known competing financial interests or personal relationships that could have appeared to influence the work reported in this paper.

Acknowledgments

This work was supported by the National Science Centre in Poland [five grants numbers: 2021/43/D/ST10/00687 (SONATA funding scheme, ŁS), 2015/19/D/ST10/02869 (SONATA funding scheme, MK), and 2017/27/B/ST10/01269 (OPUS funding scheme, KM), 2020/39/I/ST10/02129 (OPUS-LAP funding scheme, MB & ŁS), and 2023/49/N/ST10/01509 (PRELUDIUM funding scheme, AW)]; statutory funds for young researchers at the University of Wroclaw [0420/2665/17, ŁS]; statutory fund of University of Wrocław in 2005–2010 (MW, HM); and Bekker Programme at the Polish National Agency for Scientific Exchange [award no. BPN/BEK/2021/1/00431, ŁS]. We would like to thank dr Adam Nawrot for consultation regarding meteorological calculations, Piotr Modzel for the installation and maintenance of the equipment, and Mr. Peter Senn for linguistic corrections of the manuscript. The study was carried out by DI, EL as part of scientific activity of the Centre for Polar Studies (University of Silesia in Katowice) with the use of research and logistic equipment (monitoring and measuring equipment, sensors, multiple AWS, GNSS receivers, snowmobiles and other supporting equipment) of the Polar Laboratory of the University of Silesia in Katowice. For the purpose of Open Access, the authors have applied a CC BY public copyright license to any Author Accepted Manuscript (AAM) version arising from this submission. We would like to thank three anonymous reviewers for the thorough review. The publication was partially financed by the Initiative Excellence – Research University program for University of Wroclaw.

Appendix A. Supplementary data

Supplementary data to this article can be found online at https://doi.org/10.1016/j.jenvman.2025.125189.

Data availability

Meteorological data used in this study are available at PANGEA (https://doi.pangaea.de/10.1594/PANGAEA.909074), hydrological data (daily discharge, water temperature, water stage) are available at Zenodo (https://zenodo.org/records/10935540).

References

Adèr, H., Mellenbergh, G.J., Hand, D.J., 2008. Advising on Research Methods: A Consultant's Companion. Johannes van Kessel Publishing, Netherlands, p. 572.
Alobaidi, M., Ouarda, T., Marpu, P., Chebana, F., 2021. Diversity-driven ANN-based ensemble framework for seasonal low-flow analysis at ungauged sites. Adv. Water Resour. 147, 103814.
An, B., et al., 2022. Process, mechanisms, and early warning of glacier collapse-induced river blocking disasters in the Yarlung Tsangpo Grand Canyon, southeastern Tibetan Plateau. Sci. Total Environ. 816, 151652.
Anghileri, D., Pianosi, F., Soncini-Sessa, R., 2014. Trend detection in seasonal data: from hydrology to water resources. J. Hydrol. 511, 171–179.
Beel, C.R., et al., 2021. Emerging dominance of summer rainfall driving High Arctic terrestrial-aquatic connectivity. Nat. Commun. 12 (1), 1448.
Beel, C.R., Lamoureux, S.F., Orwin, J.F., 2018. Fluvial response to a period of hydrometeorological change and landscape disturbance in the Canadian High Arctic. Geophys. Res. Lett. 45 (19), 455, 10,446-10.
Beel, C.R., et al., 2020. Differential impact of thermal and physical permafrost disturbances on High Arctic dissolved and particulate fluvial fluxes. Sci. Rep. 10 (1), 11836.
Behrangi, A., Nguyen, H., Granger, S., 2015. Probabilistic seasonal prediction of meteorological drought using the bootstrap and multivariate information. J. Appl. Meteorol. Climatol. 54 (7), 1510–1522.
Beniston, M., et al., 2018. The European mountain cryosphere: a review of its current state, trends, and future challenges. Cryosphere 12 (2), 759–794.
Biecek, P., 2018. DALEX: explainers for complex predictive models in R. J. Mach. Learn. Res. 19, 1–5.
Bintanja, R., Andry, O., 2017. Towards a rain-dominated Arctic. Nat. Clim. Change 7 (4), 263–267.
Błaszczyk, M., et al., 2019a. Quality assessment and glaciological applications of digital elevation models derived from space-borne and aerial images over two tidewater glaciers of southern spitsbergen. Remote Sens. 11 (9), 1121.
Błaszczyk, M., et al., 2019b. Freshwater input to the arctic fjord Hornsund (svalbard). Polar Res. 38.
Brázdil, R., et al., 1988. Results of Investigations of the Geographical Research Expedition Spitsbergen 1985. Univerzita J/E/Purkyně v Brně, Brno, p. 337.
Brázdil, R., Piasecki, J., Prošek, P., Szczepankiewicz-Szmyrka, A., 1989. Temperature conditions and energy balance of the active surface of a moraine and maritime terrace in the Werenskiold area. Acta Universitatis Wratislaviensis No. 1069 Results of investigations ot the polish scientific Spitsbergen expeditions 7, 5–44.
Breiman, L., 2001. Random forests. Mach. Learn. 45 (1), 5–32.
Caine, N., 2010. Recent hydrologic change in a Colorado alpine basin: an indicator of permafrost thaw? Ann. Glaciol. 51 (56), 130–134.
Canty, A., Ripley, B.D., 2021. Boot: Bootstrap R (S-Plus) Functions.
Chai, Y., et al., 2022. Constrained CMIP6 projections indicate less warming and a slower increase in water availability across Asia. Nat. Commun. 13 (1), 4124.
Cooper, M.G., et al., 2023. Detecting permafrost active layer thickness change from nonlinear baseflow recession. Water Resour. Res. 59 (1), e2022WR033154.
Czerny, J., Kieres, A., Manecki, M., Rajchel, J., 1992a. Geological Map of the SW Part of Wedel-Jarlsberg Land, Spitsbergen. Institute of Geology and Mineral Deposits, University of Mining and Metallurgy. Kraków, Poland.
Czerny, J., Lipień, G., Manecki, A., Piestrzyński, A., 1992b. Geology and ore-mineralization of the hecla hoek succession (Precambrian) in front of Werenskioldbreen, south spitsbergen. Stud. Geol. Pol. 98, 67–113.
Davison, A.C., Hinkley, D.V., 1997. Bootstrap Methods and Their Applications. Cambridge University Press, Cambridge.

Debolskiy, M.V., et al., 2021. Water balance response of permafrost-affected watersheds to changes in air temperatures. Environ. Res. Lett. 16 (8), 084054.
Dobricic, S., Russo, S., Pozzoli, L., Wilson, J., Vignati, E., 2020. Increasing occurrence of heat waves in the terrestrial Arctic. Environ. Res. Lett. 15 (2), 024022.
Dobriyal, P., Badola, R., Tuboi, C., Hussain, S.A., 2017. A review of methods for monitoring streamflow for sustainable water resource management. Appl. Water Sci. 7 (6), 2617–2628.
Dunn, P.K., 2001. Bootstrap confidence intervals for predicted rainfall quantiles. Int. J. Climatol. 21 (1), 89–94.
Efron, B., 1979. Bootstrap methods: another look at the jackknife. Ann. Stat. 7 (1), 1–26.
Efron, B., Tibshirani, R.J., 1994. An Introduction to the Bootstrap, first ed. Chapman and Hall/CRC, New York.
Emmer, A., et al., 2022. Progress and challenges in glacial lake outburst flood research (2017–2021): a research community perspective. Nat. Hazards Earth Syst. Sci. 22 (9), 3041–3061.
England, M.R., Eisenman, I., Lutsko, N.J., Wagner, T.J.W., 2021. The recent emergence of arctic amplification. Geophys. Res. Lett. 48 (15), e2021GL094086.
Evans, S., Yokeley, B., Stephens, C., Brewer, B., 2020. Potential mechanistic causes of increased baseflow across northern Eurasia catchments underlain by permafrost. Hydrol. Process. 34.
Evans, S.G., Ge, S., Liang, S., 2015. Analysis of groundwater flow in mountainous, headwater catchments with permafrost. Water Resour. Res. 51 (12), 9564–9576.
Feng, D., et al., 2021. Recent changes to Arctic river discharge. Nat. Commun. 12 (1), 6917.
Førland, E.J., Benestad, R., Hanssen-Bauer, I., Haugen, J.E., Skaugen, T.E., 2011. Temperature and precipitation development at Svalbard 1900–2100. Adv. Meteorol., 893790
Ge, S., McKenzie, J., Voss, C., Wu, Q., 2011. Exchange of groundwater and surface-water mediated by permafrost response to seasonal and long term air temperature variation. Geophys. Res. Lett. 38 (14).
Ghorbani, M.A., Khatibi, R., Karimi, V., Yaseen, Z.M., Zounemat-Kermani, M., 2018. Learning from multiple models using artificial intelligence to improve model prediction accuracies: application to river flows. Water Resour. Manag. 32 (13), 4201–4215.
Górniak, D., Marszałek, H., Jankowska, K., Dunalska, J., 2016. Bacterial community succession in an arctic lake-stream system (Brattegg valley, SW Spitsbergen). Boreal Environ. Res. 21 (1–2), 115–133.
Graham, R.M., et al., 2017. Increasing frequency and duration of Arctic winter warming events. Geophys. Res. Lett. 44 (13), 6974–6983.
Hanssen-Bauer, I., et al., 2019. Climate in Svalbard 2100 Editors -a Knowledge Base for Climate Adaptation. Norwegian Centre for Climate Services, p. 208.
Harrison, S., et al., 2018. Climate change and the global pattern of moraine-dammed glacial lake outburst floods. Cryosphere 12 (4), 1195–1209.
Hipel, K.W., McLeod, A.I., 1994. Time Series Modelling of Water Resources and Environmental Systems. Elsevier Science, p. 1012.
Hollister, J., Stachelek, J., 2017. lakemorpho: calculating lake morphometry metrics in R. F1000Res 6, 1718.
Hu, X.-M., Ma, J.-R., Ying, J., Cai, M., Kong, Y.-Q., 2021. Inferring future warming in the Arctic from the observed global warming trend and CMIP6 simulations. Adv. Clim. Change Res. 12 (4), 499–507.
Huggel, C., Clague, J.J., Korup, O., 2012. Is climate change responsible for changing landslide activity in high mountains? Earth Surf. Process. Landf. 37 (1), 77–91.
Ignatiuk, D., et al., 2022. A decade of glaciological and meteorological observations in the Arctic (Werenskioldbreen, Svalbard). Earth Syst. Sci. Data 14 (5), 2487–2500.
Jakob, M., 2022. Chapter 14 - landslides in a changing climate. In: Davies, T., Rosser, N., Shroder, J.F. (Eds.), Landslide Hazards, Risks, and Disasters, second ed. Elsevier, pp. 505–579.
Jania, J., Pulina, M., 1994. Polish hydrological studies in Spitsbergen, Svalbard: a review of some results. In: Sand, K., Killingtveit, Å. (Eds.), Proceedings of the 10th International Northern Research Basins Symposium and Workshop, Spitsbergen, Norway. Norwegian Institute of Technology, Trondheim, pp. 47–76.
Kasprzak, M., 2015. High-resolution electrical resistivity tomography applied to patterned ground, Wedel Jarlsberg Land, south-west Spitsbergen. Polar Res. 34 (1), 25678.
Kasprzak, M., 2020. Seawater intrusion on the Arctic coast (Svalbard): the concept of onshore-permafrost wedge. Geosciences 10, 1–11.
Kasprzak, M., Szymanowski, M., 2023. Spatial and temporal patterns of near-surface ground temperature in the Arctic mountain catchment. Land Degrad. Dev. 34 (17), 5238–5258.
Killingtveit, Å., Pettersson, L.-E., Sand, K., 2003. Water balance investigations in Svalbard. Polar Res. 22, 161–174.
Korabiewski, B., 2023. Relict and contemporary soils on uplifted marine terraces of Kvartsittsletta, SW Spitsbergen. Pol. Polar Res. 44 (3), 249–269.
Krogh, S.A., Pomeroy, J.W., 2018. Recent changes to the hydrological cycle of an Arctic basin at the tundra–taiga transition. Hydrol. Earth Syst. Sci. 22 (7), 3993–4014.
Kuhn, M., 2008. Building predictive models in R using the caret package. J. Stat. Software 28 (5), 1–26.
Kumar, B., Prabhu, T.S.M., Sathyan, A., Krishnan, A., 2022. Chapter 36 - GLOF early warning system: computational challenges and solutions. In: Zakwan, M., Wahid, A., Niazkar, M., Chatterjee, U. (Eds.), Current Directions in Water Scarcity Research. Elsevier, pp. 641–662.
Kundzewicz, Z.W., Robson, A.J., 2004. Change detection in hydrological records—a review of the methodology/Revue méthodologique de la détection de changements dans les chroniques hydrologiques. Hydrol. Sci. J. 49 (1), 7–19.
Kurylyk, B., Hayashi, M., Quinton, W., McKenzie, J., Voss, C., 2016. Influence of vertical and lateral heat transfer on permafrost thaw, peatland landscape transition, and groundwater flow. Water Resour. Res. 52, 1286–1305.
Lafrenière, M.J., Lamoureux, S.F., 2019. Effects of changing permafrost conditions on hydrological processes and fluvial fluxes. Earth Sci. Rev. 191, 212–223.
Lamhonwah, D., Lafrenière, M.J., Lamoureux, S.F., Wolfe, B.B., 2017. Evaluating the hydrological and hydrochemical responses of a High Arctic catchment during an exceptionally warm summer. Hydrol. Process. 31 (12), 2296–2313.
Lamontagne-Hallé, P., McKenzie, J., Kurylyk, B., Zipper, S., 2018. Changing groundwater discharge dynamics in permafrost regions. Environ. Res. Lett. 13.
Lehmann-Konera, S., Ruman, M., Kozioł, K., Gajek, G., Polkowska, Ż., 2017. Glaciers as an important element of the world glacier monitoring implemented in svalbard. In: Godone, D. (Ed.), Glacier Evolution in a Changing World. Intech Open, pp. 1–36.
Lewis, T., Lafrenière, M.J., Lamoureux, S.F., 2012. Hydrochemical and sedimentary responses of paired High Arctic watersheds to unusual climate and permafrost disturbance, Cape Bounty, Melville Island, Canada. Hydrol. Process. 26 (13), 2003–2018.
Lewis, T., Lamoureux, S.F., 2010. Twenty-first century discharge and sediment yield predictions in a small high Arctic watershed. Global Planet. Change 71 (1–2), 27–41.
Li, Z., Chen, Y., Li, Y., Wang, Y., 2020. Declining snowfall fraction in the alpine regions, Central Asia. Sci. Rep. 10 (1), 3476.
Lin, L., et al., 2020. Understanding the effects of climate warming on streamflow and active groundwater storage in an alpine catchment: the upper Lhasa River. Hydrol. Earth Syst. Sci. 24 (3), 1145–1157.
Lützow, N., Veh, G., Korup, O., 2023. A global database of historic glacier lake outburst floods. Earth Syst. Sci. Data 15 (7), 2983–3000.
Łupikasza, E., et al., 2019. The role of winter rain in the glacial system on svalbard. Water 11, 334.
Łupikasza, E., Niedzwiedz, T., Przybylak, R., Nordli, Ø., 2021. Importance of regional indices of atmospheric circulation for periods of warming and cooling in svalbard during 1920–2018. Int. J. Climatol. 41, 3481–3502.
Majchrowska, E., Ignatiuk, D., Jania, J., Marszałek, H., Wąsik, M., 2015. Seasonal and interannual variability in runoff from the Werenskioldbreen catchment, Spitsbergen. Pol. Polar Res. 36 (3), 197–224.
Makarieva, O., Nesterova, N., Post, D., Sherstiukov, A., Lebedeva, L., 2019. Warming temperatures are impacting the hydrometeorological regime of Russian rivers in the zone of continuous permafrost. Cryosphere 13, 1635–1659.
Marszałek, H., Górniak, D., 2017. Changes in water chemistry along the newly formed High Arctic fluvial–lacustrine system of the Brattegg Valley (SW Spitsbergen, Svalbard). Environ. Earth Sci. 76 (13), 449.
Marszałek, H., Wąsik, M., 2013. Some physico-chemical features of water in suprapermaforst zone in the Hornsund region (SW Spitsbergen). Biul. Panstwowego Inst. Geol. (1989) 456, 497, 404.
McCrystall, M.R., Stroeve, J., Serreze, M., Forbes, B.C., Screen, J.A., 2021. New climate models reveal faster and larger increases in Arctic precipitation than previously projected. Nat. Commun. 12 (1), 6765.
Migała, K., et al., 2023. Climate indices of environmental change in the high arctic: study from Hornsund, SW spitsbergen, 1979–2019. Pol. Polar Res. 44 (2 : Special Issue to celebrate 50 years anniversary of Stanislaw Baranowski Polar Station in Spitsbergen: Part 1), 91–126.
Migała, K., et al., 2013. Geographical environment in the vicinity of the stanislaw Baranowski polar station – werenskioldbreen. In: Zwoliński, Z., Kostrzewski, A., Pulina, M. (Eds.), Ancient and Modern Geoecosystems of Spitsbergen. Association of Polish Geomorphologists, Poznań, Poland, pp. 101–144.
Migała, K., Piasecki, J., Pereyma, J., 2015. Dorobek ośrodka wrocławskiego w meteorologii i klimatologii obszarów polarnych. Probl. Klimatol. Polarnej 25, 9–18.
Moholdt, G., Wesselink, D., Aas, H.F., 2019. Merged Svalbard Digital Terrain Model [database]. Norwegian Polar Institute.
Nakamura, T., Sato, T., 2022. A possible linkage of Eurasian heat wave and East Asian heavy rainfall in Relation to the Rapid Arctic warming. Environ. Res. 209, 112881.
Nowak, A., Hodgkins, R., Nikulina, A., Osuch, M., Wawrzyniak, T., Kavan, J., Łepkowska, E., Majerska, M., Romashova, K., Vasilevich, I., Sobota, I., Rachlewicz, G., 2021. From land to fjords: The review of Svalbard hydrology from 1970 to 2019 (SvalHydro), in: SESS report 2020 - The State of Environmental Science in Svalbard - an annual report. Svalbard Integrated Arctic Earth Observing, pp. 176–201. System. https://doi.org/10.5281/zenodo.4294063.
Nowak, A., Hodson, A., 2013. Hydrological response of a High-Arctic catchment to changing climate over the past 35 years: a case study of Bayelva watershed, Svalbard. Polar Res. 32 (Suppl. L), 19691.
Osuch, M., Wawrzyniak, T., Łepkowska, E., 2022. Changes in the flow regime of High Arctic catchments with different stages of glaciation, SW Spitsbergen. Sci. Total Environ. 817, 152924.
Osuch, M., Wawrzyniak, T., Nawrot, A., 2019. Diagnosis of the hydrology of a small Arctic permafrost catchment using HBV conceptual rainfall-runoff model. Nord. Hydrol. 50 (2), 459–478.
Owczarek, P., Nawrot, A., Migala, K., Malik, I., Korabiewski, B., 2014. Flood-plain responses to contemporary climate change in small High-Arctic basins (Svalbard, Norway). Boreas 43 (2), 384–402.
Owczarek, P., Opała-Owczarek, M., Boudreau, S., Lajeunesse, P., Stachnik, Ł., 2020. Re-activation of landslide in sub-Arctic areas due to extreme rainfall and discharge events (the mouth of the Great Whale River, Nunavik, Canada). Sci. Total Environ., 140991
Owczarek, P., Opała-Owczarek, M., Migala, K., 2021. Post-1980s shift in the sensitivity of tundra vegetation to climate revealed by the first dendrochronological record from Bear Island (Bjørnøya), western Barents Sea. Environ. Res. Lett. 16, 014031.

Park, H., Kim, Y., Suzuki, K., Hiyama, T., 2024. Influence of snowmelt on increasing Arctic river discharge: numerical evaluation. Prog. Earth Planet. Sci. 11 (1), 13.
Pedersen, Å.Ø., et al., 2022. Five decades of terrestrial and freshwater research at Ny-Ålesund, Svalbard. Polar Res. 41.
Pelt, W.V., Kohler, J., 2015. Modelling the long-term mass balance and firn evolution of glaciers around Kongsfjorden, Svalbard. J. Glaciol. 61 (228), 731–744.
Piasecki, J., Pulina, M., 1975. Przepływ rzeki lodowcowej Werenskiolda i rzeki Brattegg jako funkcja niektórych parametrów klimatycznych w 1972, in: Polskie wyprawy na Spitsbergen 1972 i 1973 r. Materiały z Sympozjum Spitsbergeńskiego. Wrocław 67–72.
Pohlert, T., 2020. Non-parametric Trend Tests and Change-point Detection.
Porter, C., et al., 2018. ArcticDEM.
Przybylak, R., Araźny, A., 2006. Climatic conditions of the north−western part of Oscar II Land (Spitsbergen) in the period between 1975 and 2000. Pol. Polar Res. 27, 133–152.
Przytulska, A., Bartosiewicz, M., Vincent, W.F., 2017. Increased risk of cyanobacterial blooms in northern high-latitude lakes through climate warming and phosphorus enrichment. Freshwater Biology 62 (12), 1986–1996.
Qin, Y., et al., 2020. Agricultural risks from changing snowmelt. Nat. Clim. Change 10 (5), 459–465.
R Core Team, 2014. A Language and Environment for Statistical Computing. R Foundation for Statistical Computing, Vienna, Austria.
Rawlins, M.A., Karmalkar, A.V., 2024. Regime shifts in Arctic terrestrial hydrology manifested from impacts of climate warming. Cryosphere 18 (3), 1033–1052.
Robison, A.L., Deluigi, N., Rolland, C., Manetti, N., Battin, T., 2023. Glacier loss and vegetation expansion alter organic and inorganic carbon dynamics in high-mountain streams. Biogeosciences 20 (12), 2301–2316.
Savin, N.E., White, K.J., 1977. The Durbin-Watson Test for Serial Correlation with Extreme Sample Sizes or Many Regressors. Econometrica 45 (8), 1989–1996.
Schmidt, L.S., Schuler, T.V., Thomas, E.E., Westermann, S., 2023. Meltwater runoff and glacier mass balance in the high Arctic: 1991–2022 simulations for Svalbard. Cryosphere 17 (7), 2941–2963.
Senderak, K., Kondracka, M., Gądek, B., 2017. Talus slope evolution under the influence of glaciers with the example of slopes near the Hans Glacier, SW Spitsbergen, Norway. Geomorphology 285, 225–234.
Senderak, K., Wąsowski, M., 2016. Chemical Weathering of Talus Slopes: the Example of Slopes in the Brattegg Valley, Sw Spitbergen, vol. 50. Studia Geomorphologica Carpatho-Balcanica, pp. 105–122.
Serreze, M., et al., 2021. Arctic rain on snow events: bridging observations to understand environmental and livelihood impacts. Environ. Res. Lett. 16.
Serreze, M.C., Crawford, A.D., Barrett, A.P., 2015. Extreme daily precipitation events at spitsbergen, an arctic Island. Int. J. Climatol. 35 (15), 4574–4588.
Shan, W., et al., 2015. The impact of climate change on landslides in southeastern of high-latitude permafrost regions of China. Front. Earth Sci. 3.
Sharma, S.K., Tiwari, K.N., 2009. Bootstrap based artificial neural network (BANN) analysis for hierarchical prediction of monthly runoff in Upper Damodar Valley Catchment. J. Hydrol. 374 (3), 209–222.
Sihag, P., Al-Janabi, A.M.S., Alomari, N.K., Ghani, A.A., Nain, S.S., 2021. Evaluation of tree regression analysis for estimation of river basin discharge. Modeling Earth Systems and Environment 7 (4), 2531–2543.
Singh, P., Ramasastri, K.S., Kumar, N., Arora, M., 2000. Correlations between discharge and meteorological parameters and runoff forecasting from a highly glacierized Himalayan basin. Hydrol. Sci. J. 45 (5), 637–652.
Sjöberg, Y., et al., 2021. Permafrost promotes Shallow groundwater flow and warmer headwater streams. Water Resour. Res. 57 (2), e2020WR027463.
Sobota, I., Weckwerth, P., Grajewski, T., 2020. Rain-On-Snow (ROS) events and their relations to snowpack and ice layer changes on small glaciers in Svalbard, the high Arctic. J. Hydrol. 590, 125279.
Song, C., Wang, G., Sun, X., Hu, Z., 2021. River runoff components change variably and respond differently to climate change in the Eurasian Arctic and Qinghai-Tibet Plateau permafrost regions. J. Hydrol. 601, 126653.
Stachniak, K., Sitek, S., Ignatiuk, D., Jania, J., 2022. Hydrogeological model of the forefield drainage system of werenskioldbreen. Svalbard. Water 14 (9), 1514.
Stachnik, Ł., et al., 2016. Chemical denudation and the role of sulfide oxidation at Werenskioldbreen, Svalbard. J. Hydrol. 538, 177–193.
Sterling, S.M., Ducharne, A., Polcher, J., 2013. The impact of global land-cover change on the terrestrial water cycle. Nat. Clim. Change 3 (4), 385–390.
Stuefer, S.L., Arp, C.D., Kane, D.L., Liljedahl, A.K., 2017. Recent extreme runoff observations from coastal Arctic watersheds in Alaska. Water Resour. Res. 53 (11), 9145–9163.
Sund, M., 2008. Polar Hydrology Norwegian Water Resources and Energy Directorate's Work in Svalbard, p. 66.
Szponar, A., 1989. Deglaciation of Spitsbergen glacier cirques in aqueous and subaqueous conditions. Acta Universitatis Wratislaviensis No. 1069 Results of investigations ot the polish scientific Spitsbergen expeditions 7, 87–93.
Taylor, C., Robinson, T.R., Dunning, S., Rachel Carr, J., Westoby, M., 2023. Glacial lake outburst floods threaten millions globally. Nat. Commun. 14 (1), 487.
van Pelt, W., et al., 2019. A long-term dataset of climatic mass balance, snow conditions, and runoff in Svalbard (1957–2018). Cryosphere 13 (9), 2259–2280.
Vonk, J.E., Speetjens, N.J., Poste, A.E., 2023. Small watersheds may play a disproportionate role in arctic land-ocean fluxes. Nat. Commun. 14 (1), 3442.
Vonk, J.E., et al., 2015. Reviews and syntheses: effects of permafrost thaw on Arctic aquatic ecosystems. Biogeosciences 12 (23), 7129–7167.
Vörösmarty, C.J., et al., 2010. Global threats to human water security and river biodiversity. Nature 467 (7315), 555–561.
Walvoord, M., Striegl, R., 2007. Increased groundwater to stream discharge from permafrost thawing in the Yukon River Basin: potential impacts on lateral export of carbon and nitrogen. Geophys. Res. Lett. 34, L12402.
Walvoord, M.A., Kurylyk, B.L., 2016. Hydrologic impacts of thawing permafrost—a review. Vadose Zone J. 15 (6) vzj2016.01.0010.
Wang, P., et al., 2021. Potential role of permafrost thaw on increasing Siberian river discharge. Environ. Res. Lett. 16, 034046.
Wang, X., et al., 2019. Changes in river discharge in typical mountain permafrost catchments, northwestern China. Quat. Int. 519, 32–41.
Wang, Z., et al., 2022. Variation characteristics of high flows and their responses to climate change in permafrost regions on the Qinghai-Tibet Plateau, China. J. Clean. Prod. 376, 134369.
Wang, G., Liu, G., Liu, L., 2012. Spatial scale effect on seasonal streamflows in permafrost catchments on the Qinghai–Tibet Plateau. Hydrol. Processes 26 (7), 973–984. https://doi.org/10.1002/hyp.8187.
Wang, Z., Sun, S., Wang, G., Song, C., 2023. Determination of low-flow components in alpine permafrost rivers. J. Hydrol. 617, 128886.
Wawrzyniak, T., Majerska, M., Osuch, M., 2020. Hydrometeorological dataset (2014-2019) from the high Arctic unglaciated catchment Fuglebekken (Svalbard). Hydrol 35, e13974.
Wawrzyniak, T., Osuch, M., 2019. A consistent high arctic climatological dataset (1979-2018) of the polish polar station Hornsund (SW spitsbergen, svalbard). In: PANGEA.
Wawrzyniak, T., Osuch, M., 2020. 40 years high arctic climatological dataset of the polish polar station Hornsund (SW spitsbergen, svalbard). Earth Syst. Sci. Data 12, 805–815.
Wawrzyniak, T., Osuch, M., Napiórkowski, J., Westermann, S., 2016. Modelling of the thermal regime of permafrost during 1990–2014 in Hornsund, Svalbard. Pol. Polar Res. 37 (2), 219.
Wąsik, M., Marszałek, H., Rysiukiewicz, M., 2023. Permeability of active layer sediments and groundwater runoff in Brattegg River catchment, SW Spitsbergen. Pol. Polar Res. 44 (No 2 : Special Issue to celebrate 50 years anniversary of Stanislaw Baranowski Polar Station in Spitsbergen: Part 1), 197–219.
Westoby, M.J., et al., 2014. Modelling outburst floods from moraine-dammed glacial lakes. Earth Sci. Rev. 134, 137–159.
WGMS, 2020. World Glacier Monitoring System [database]. (Accessed 7 December 2020).
Wickström, S., Jonassen, M.O., Cassano, J.J., Vihma, T., 2020. Present temperature, precipitation, and rain-on-snow climate in Svalbard. J. Geophys. Res. Atmos. 125 (14), e2019JD032155.
Wilcox, R., 2001. Fundamentals of Modern Statistical Methods: Substantially Improving Power and Accuracy.
Wołoszyn, A., Kasprzak, M., 2023. Contemporary landscape transformation in a small Arctic catchment, Bratteggdalen, Svalbard. Pol. Polar Res. 44, 227–248.
Young, K.L., Lafrenière, M.J., Lamoureux, S.F., Abnizova, A., Miller, E.A., 2015. Recent multi-year streamflow regimes and water budgets of hillslope catchments in the Canadian High Arctic: evaluation and comparison to other small Arctic watershed studies. Nord. Hydrol 46 (4), 533–550.
Zastruzny, S.F., Ingeman-Nielsen, T., Zhang, W., Elberling, B., 2023. Accelerated permafrost thaw and increased drainage in the active layer: responses from experimental surface alteration. Cold Reg. Sci. Technol. 212, 103899.
Zastruzny, S.F., Sjöberg, Y., Jensen, K.H., Liu, Y., Elberling, B., 2024. Impact of Summer Air Temperature on Water and Solute Transport on a Permafrost-Affected Slope in West. Greenland. Water Resour. Res. 60 (11), e2023WR036147. https://doi.org/10.1029/2023WR036147.
Zhou, J., Peng, T., Zhang, C., Sun, N., 2018. Data pre-analysis and ensemble of various artificial neural networks for monthly streamflow forecasting. Water 10 (5), 628.
Zhu, B., et al., 2023. Constrained tropical land temperature-precipitation sensitivity reveals decreasing evapotranspiration and faster vegetation greening in CMIP6 projections. npj Climate and Atmospheric Science 6 (1), 91.
Zounemat-Kermani, M., Batelaan, O., Fadaee, M., Hinkelmann, R., 2021. Ensemble machine learning paradigms in hydrology: a review. J. Hydrol. 598, 126266.